공학박사학위논문

Superstructure Optimization of Low Temperature Organic Rankine Cycle with Multi Component Working Fluid

다성분 작동유체를 이용한 저온 랭킨 사이클의 초구조체 최적화

2016년 8월

서울대학교 대학원

화학생물공학부

전 정 우

Abstract

Superstructure Optimization of Low Temperature Organic Rankine Cycle with Multi Component Working Fluid

Jeongwoo Jeon

School of Chemical & Biological Engineering

The Graduate School of Seoul National University

Liquefied natural gas (LNG) has been receiving attention as energy source because of its high-energy density and low emission of greenhouse gas problems. Typically, LNG is evaporated by sea water in LNG terminal without using its cryogenic energy. The cryogenic energy of LNG can be utilized for power generation using organic Rankine cycle (ORC). In this thesis, an optimal ORC process utilizing LNG cold energy is proposed. The ORC process is modeled using commercial process simulator. The working fluid of the ORC is composed of normal pentane, trifluoromethane, and tetrafluoromethane. The optimization of the process to minimize total annualized cost (TAC) is performed using superstructure based approach. The developed superstructure includes four process alternatives, which are MSCHE, vapor flash process, 2-stage expansion, and VRP. The optimum solution is attained using the process simulator-interface-optimizer structure. As a

result of optimization, the optimum ORC process configuration including MSCHE and 2-stage expansion is obtained. The optimal process shows the net power generation of 409.6 GJ/h, and the power generation per unit kilogram of LNG is increased by 68.2 %.

Keywords: LNG, Multi Component Working Fluid, Organic Rankine Cycle, Superstructure, Genetic Algorithm

Student ID: 2009-21023

Contents

List of Figures

List of Tables

CHAPTER 1 : Introduction

1.1. Research motivation

Liquefied natural gas (LNG) has been receiving attention as energy source because of its high-energy density and low emission of greenhouse gas problems. Typically, LNG is evaporated in gaseous phase in LNG terminal to transport natural gas to final consumers. In most cases, LNG is evaporated using sea water in open rack vaporizer (ORV), thus cryogenic energy of LNG is mostly wasted which could be utilized for other purposes. The cryogenic energy of LNG can be utilized mainly for power generation, air separation, and CO2 liquefaction etc [1].

The power generation which is using organic Rankine cycle (ORC) is one of the best way of recovering that wasted cryogenic energy of LNG. Because ORCs use organic compounds as their working fluids and operate in wide temperature range, the cryogenic energy of LNG can be effectively utilized in ORCs.

1.2. Research objectives

Many researches have been conducted onto design and optimization of ORC. There are three major issues when designing and optimizing ORCs: selecting working fluid, choosing heat sources, and deciding cycle configurations.

The selection of the working fluid may have predominant effect of thermodynamic and economic performance of the ORCs. Several hundreds of researches focused on the selection of pure substance as a working fluid [2-12]. In these researches, hydrocarbons and halogenated carbons were mainly considered and evaluated to find the most effective working fluid for the cycle. However, non-isothermal evaporation nature of LNG introduces temperature pinch during the evaporation when pure species are used as working fluid. The temperature pinch results high exergy loss during the working fluid condensation and consequently, reduces power generation from the ORC. Multi component working fluids can make temperature difference, called as temperature glide, smaller than pure substances during condensation and reduce exergy loss. Liu and Guo [13] proposed a novel cryogenic cycle with a vapor absorption process using a binary mixture as working fluids. Propane and tetrafluoromethane were employed as the working fluid and the performance of the power cycle was increased by 66.3% compared to conventional propane ORC. Kim et al. [14] suggested binary mixture working fluid in cascade ORC utilizing LNG cold energy. Optimum working fluid combination and process configuration were obtained through optimization, and the proposed cycle generated 157.76 kJ per kg LNG under a 25 °C heat source. Sun et al. [15] proposed a novel Rankine power cycle that uses a ternary hydrocarbon mixture as working fluid to recover the cold energy of LNG. They discovered that the ethylene is more appropriate than ethane to be used in the mixed working fluid. With LNG direct expansion, proposed cycle could output 1.346 kWh of work for 1 kmol of LNG. Shi and Che [16] proposed a combined power system utilizing both low-temperature waste heat and cold energy of LNG. This system was made up of an ammonia-water mixture Rankine cycle and an LNG power generation cycle. The results showed a

net electrical efficiency of 33%. A parametric analysis was also performed, and the maximum net electrical efficiency could be obtained as the inlet pressure of ammonia turbine and the ammonia mass fraction increased. Wang et al. [17] also presented an ammonia-water power system with LNG as its heat sink. They performed multi-objective optimization consists of the exergy efficiency, total heat transfer capability, and turbine size to find optimum system performance. Lee et al. [18] suggested ternary organic mixtures and Heberle et al. [19] proposed zeotropic mixtures as working fluids to enhance the cycle efficiency.

The power generation efficiency of the cycle is greatly influenced by the choice of heat source. Waste heat [2] (steam or flue gases), solar energy [20] and geothermal heat [21] can be the heat source of the ORCs. Waste heat recovery applications are mainly composed of the low temperatures (<350 ℃) and the low heat content [22]. Wang et al. [17] adopted exhaust gas of 200 ℃ as a low-grade waste heat source. Roy et al. [23] utilized the flue gas having temperature of 140 ℃, as a heat source. They performed parametric study and performance analysis for the waste heat recovery ORC. The result showed that the power generation of the cycle can reaches 19.09 MW with R-123 working fluid. Lee et al. [24] proposed combined Rankine cycle using LNG and low grade steam of a coal power plant, and the net power generation was improved by 73% compared to a conventional power cycle. Zhao et al. [25] introduced a novel system based on LNG cold energy utilization for capturing CO2. Through a combination with twin-stage ORC power generation sub-system using LNG as heat sink and exhaust gas as heat source, the system could produce maximum network output of 119.42 kW. Heberle et al. [19] used geothermal heat sources under 120 ℃ for power generation of ORC. Madhawa Hettiarachchi et al. [26] utilized the power generating potential of low-temperature

geothermal resources in the range of 70 – 100 °C. In addition, several studies have been conducted using solar energy as a heat source for power generation of ORCs [20, 27].

The design of novel Rankine cycle configuration is another major issue in ORC research. Several authors introduced a recuperator to improve cycle efficiency [4, 28, 29]. A recuperator enables the coldness of the working fluid or the heat after the expander to be reused. It is known that a recuperator essentially increases the thermal efficiency of the cycle [4]. Consequently, a recuperator can improve the power generation of the ORCs. Some other studies suggested regenerative ORCs [30-33]. In a regenerative ORC, the turbine bleeding and direct contact heater are used thus working fluid flow rate is increased resulting higher power generation. This type of cycles resemble the ORC with recuperator in aspect of preheating of working fluid before entering the evaporator. A regenerative ORC shows a result of higher thermal efficiency than a basic ORC. Lee and Han [29] proposed and optimized a multi-component working fluid organic Rankine cycle with advanced configuration using LNG and waste heat of CO_2 capture process. Through the advanced configurations; working fluid recuperation and vapor recondensation; power generation efficiency was increased. The proposed cycle could produce 304 kJ per kg LNG, and its 2nd law efficiency was 46.2%. A number of studies proposed organic flash cycle (OFC) [34-36]. In the OFC, working fluids are depressurized in the flash tank or partially evaporated. The vapor fraction is fed to a turbine, while the liquid fraction is directly returned to the condenser or flashed further and produced vapor is fed to a low pressure turbine. More power generation is available through OFCs because different pressure-level expansion of the working fluids produce more vapor. Meanwhile, Łukasz and Maciej [37] introduced an absorption

cycle coupled with propane ORC to utilize the LNG cold exergy.

Recently, simultaneous optimization of working fluid and process configuration is also carried out. Lampe et al. [38] suggested a framework for the simultaneous optimization of working fluid and process for the ORC using geothermal heat source. PC-SAFT equation of state with continuous-molecular targeting-computer aided molecular design (CoMT-CAMD) predicts thermophysical properties of working fluids. Simultaneous optimization of ORC is active and promising research area. However, it often requires expensive calculation time and fails to global optimum solution.

The superstructure optimization can be used to find the optimum structure of ORC. A superstructure has most of alternative process configurations that a system can have. To find the optimal process configuration in a given superstructure, mixed integer non-linear programming (MINLP) has been widely used [39-41]. In the superstructure optimization, the selection of process alternatives are modeled using binary variables, and the process properties are modeled using continuous variables.

Herein, an ORC utilizing LNG cold energy with multi component working fluid was proposed and optimized. The superstructure contains 9 possible process configurations and modeled using Aspen Plus. The process alternatives are selected considering process characteristics and process improving potential. By selecting process alternatives only with high process improving potential, the total number of process alternatives contained in a superstructure can be decreased. As the size and complexity of superstructure are reduced, the superstructure optimization can be performed by commercial optimization solvers. The superstructure optimization is

performed using a Genetic Algorithm (GA) built in MATLAB. The process model is developed using Aspen Plus and the process alternatives are evaluated through Aspen Plus-interface-MATLAB GA optimizer. This decomposition between process modeling and optimization can help the process simulator to handle the complexity of process simulation only. Accordingly, the superstructure optimization problem can be simplified. To obtain the maximum power generation of the ORC, the process configuration and the pressure of the working fluid are optimized through this framework.

1.3. Outline of the thesis

The thesis is organized as follows. Chapter 1 provides motivation and objectives of this study. Chapter 2 describes the basic ORC and the design of ORC superstructure. The superstructure is developed using commercial process simulator. In the superstructure, process alternatives which can improve the efficiency of ORC are employed. In chapter 3, an optimization problem is formulated to find the optimum process configuration and operating condition. The superstructure optimization is performed using genetic algorithm built in MATLAB. Chapter 4 addresses the result of optimization. The result is analyzed and verified by sensitivity analysis. The proposed ORC process configuration shows better efficiency than the base case. Chapter 5 deals with the design of ship vapor recovery unit (SVRU). Through the process modification, the efficiency of the process is improved. Finally, chapter 6 presents the conclusion and the recommendation for

future works.

CHAPTER 2 : Process Description and Superstructure Design

2.1. Base case

The basic ORC is selected as a base case of this study because of its simplicity. The process improving potential of each process alternatives can be compared and evaluated effectively with the basic ORC. The process scheme of the basic ORC is shown in Figure 2-1. The basic ORC consists of a condenser, a pump, an evaporator, and a turbine. The working fluid and the LNG are pressurized through pumps. In the evaporator, the working fluid is heated up to the state of superheated vapor by given heat source. The working fluid is sent to the turbine after heating. In the turbine, the working fluid expands and produces mechanical work. This shaft work can be converted to electricity by the generator. The working fluid from the turbine is condensed to liquid by the LNG. The liquid working fluid is sent back to the pump to complete the cycle.

Process modeling and simulation of the ORCs is carried out using Aspen Plus™ v7.3. The Peng-Robinson [42] equation of state is used to calculate the thermodynamic properties and phase behavior of the ORCs. The Peng-Robinson equation of state is commonly used to describe the thermodynamic behavior of hydrocarbons and refrigerants [13, 18]. The composition of LNG adopted as a heat sink is summarized in Table 2-1. The mass flow rate of LNG is assumed to be 1620

tonne/h, corresponding to the regasification process operation at the Incheon LNG terminal in South Korea [29]. LNG is pressurized to 30 bar and fully vaporized in the condenser. Throughout the whole process modeling, the minimum temperature approaches of the heat exchangers are set up to 5 °C and the pressure drops of the process units (heat exchangers, flash drum, and pipelines) are neglected. Some other assumptions are made during process modeling of the ORCs. The isentropic efficiencies of turbines are set up to 72%, which is a default value of the Aspen Plus. It is assumed that the evaporators and reheaters in the ORCs use the free heat source at 100 °C such as waste heat or geothermal energy. The ORCs in this thesis uses a ternary component mixture as a working fluid. The working fluid consists of normal pentane, tetrafluoromethane, and trifluoromethane [29]. The composition of the working fluid is shown in Table 2-2.

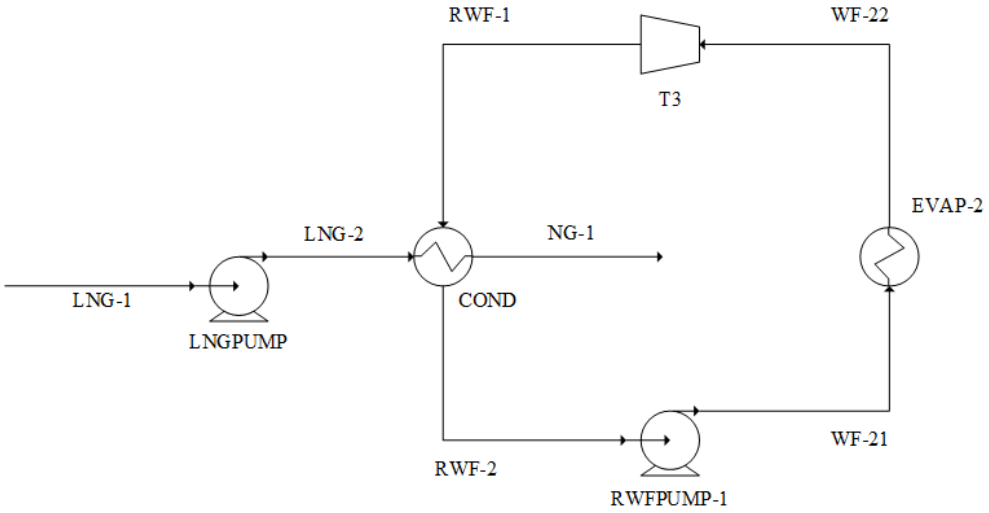

Figure 2-1. Process scheme of the basic ORC

Table 2-1. Composition of LNG

Component	Mole Fraction
N2	0.0007
CH4	0.8877
C2H6	0.0754
C3H8	0.0259
n-C4H8	0.0056
i-C4H8	0.0045
n-C5H12	0.0001
i-C5H12	0.0001
Total	1

Table 2-2. Composition of the working fluid

Component	Mass Fraction
Normal Pentane	0.09
Tetrafluoromethane	0.33
Trifluoromethane	0.58
Total	1

2.2. Process Alternatives and Superstructure Design

Several process alternatives can be implemented in the design of the ORCs in order to maximize the power generation. Process alternatives include multi-stream cryogenic heat exchanger (MSCHE), vapor flash, 2-stage expansion, and vapor recondensation process (VRP). The superstructure model contains all of aforementioned process configurations. Figure 2-2 depicts the developed superstructure of the ORC.

The MSCHE can be used in place of condenser in the base case for condensation of working fluid to maximize the use of LNG cold energy. MSCHEs are widely used in LNG liquefaction process with mixed refrigerants [43]. The liquid working fluid outlet (WF-3) of the first working fluid pump (WFPUMP-1) is colder than the vapor inlet stream (WF-1) of the MSCHE. Thus, the WF-3 stream can be utilized in company with the LNG for the condensation of the working fluid. As a result, the amount of heat sink and the mass flow rate of the working fluid can be increased with a fixed amount of LNG. This can increase the amount of power generation in turbine also. In the superstructure, the ORC configuration with MSCHE can be selected at the SP1, which is modeled as a stream selector module in the Aspen Plus. When SP1 has a value of 0, the ORC choose the MSCHE configuration. On the other hand, the typical condenser (COND) is selected when the value of SP1 is 1.

Typically, the working fluid outlet exhausted from MSCHE (WF-2) is at the saturated liquid state. The vapor flash can make the vapor fraction in the working fluid outlet stream (WF-4) of the MSCHE. In the superstructure, the ORC

configuration with vapor flash can be selected at the SP2, which is modeled as a splitter in the Aspen Plus. When the value of SP2 is 1, the ORC choose the vapor flash configuration. In this configuration, additional flash drum is required. The vapor fraction is generated in WF-4 as the discharge pressure of the WFPUMP-1 goes down. The working fluid containing vapor fraction is flashed in the flash drum (FLASH). The vapor fraction of the working fluid is heated up to 95 °C at the reheater (RH-1) and sent to the turbine for power generation. While, the liquid fraction of the working fluid goes to the second working fluid pump (WFPUMP-2) for further pressurization and power generation. The critical value of WFPUMP-1 discharge pressure for making vapor fraction in WF-4 is 17.6 bar. The lower bound of discharge pressure of WFPUMP-1 is set to 5 bar to secure power generation of the first stage turbine (T1). The operating range of discharge pressure of WFPUMP-1 (5 bar to 17.6 bar) in vapor flash configuration is sufficient to generate power from turbine expansion because the minimum pressure ratio is over 3. This configuration can reduce the power consumptions of the working fluid pumps.

The 2-stage expansion is inevitable for vapor recondensation process. In the superstructure, the ORC configuration with 2-stage expansion can be selected at the SP3, which is modeled as a splitter in the Aspen Plus. When SP3 has a value of 1, the ORC choose the 2-stage expansion configuration. While the 1-stage expansion configuration is selected, when the value of SP3 is 0. In the 2-stage expansion configuration, the exhausted stream from the first stage turbine (T1) is heated up to 95 °C again in the reheater (RH-1) and sent to the second stage turbine (T2). This eventually increases the amount of power generation. However, this configuration needs more turbine and reheater, resulting more expensive cost of process.

When the number of stage of expansion is increased, the amount of power generation can be increased also. Because the more stage is adapted, the more heat source can be utilized by reheaters. However, with only 2-stage expansion, the pressure of working fluid can be reached near the upper bound. Moreover, the increment of power generation caused by additional expansion stage is too small to overcome the increment of process cost caused by more turbines, pumps, and reheaters. Therefore, multi-stage expansion, with 3 stages or more, is not considered as a process alternative in this study.

The vapor recondensation process can be employed to the ORC in order to recuperate liquefied cryogenic working fluid. VRP is used generally to handle boil-off gas of LNG terminals [44]. In the superstructure, the VRP configuration can be selected at the SP4, which is modeled as a splitter in the Aspen Plus. When SP4 has a value of 1, the ORC choose the VRP configuration. The pressurized working fluid from a condenser (WF-6) is at the state of subcooled. Thus, the fraction of the outlet stream from the first stage turbine (WF-20) can be liquefied by mixing with the subcooled working fluid in the direct contact heater (DCH). By the direct mixing, the vapor stream can be fully liquefied (WF-10) and sent to the second working fluid pump (WFPUMP-2) for further processing. In this procedure, the split fraction of the WF-15 stream is calculated by the design spec of the Aspen Plus to set the WF-10 stream in fully liquefied state. As a result of this process configuration, the mass flow rate of the working fluid passing through the turbine and the amount of power generation can be increased.

Natural gas (NG-1) which is fully vaporized in the condenser has the temperature of -31.3 °C. It is needed to be heated further in order to supply to the final

consumers. Generally, this natural gas is heated up to around 30 ℃ by the natural gas heater, and this process requires additional heat duty. By introducing natural gas preheater (NGPREH), vaporized natural gas can be preheated before sending to the natural gas heater. The expanded working fluid (WF-24) from the turbine is at the superheated state. In the NGPREH, heat exchange between superheated working fluid and vaporized natural gas occurs. The excess heat of the working fluid is transferred to the natural gas through this heat exchange. By this process, the heat duty of natural gas can be reduced.

The decision variables and its bounds are summarized in Table 2-3. The continuous decision variables of the superstructure are discharge pressure of the first and second working fluid pump (WFPUMP-1, WFPUMP-2). The lower and upper bound of $P_{WFPUMP-1}$ are 5 bar and 34.7 bar. That of $P_{WFPUMP-2}$ is 17.6 bar and 90 bar. The upper bound of $P_{WFPUMP-2}$ is set to avoid too much liquid fraction in the turbine outlet stream. When $P_{WFPUMP-2}$ is at the condition of upper bound (90 bar), liquid fraction in the turbine outlet stream (WF-14) is 5 – 7 %. In general, permissible level of liquid fraction in turbine outlet is 5 – 10 %. In VRP and vapor flash process configuration, the intermediate pressure working fluid vapor generated from the first stage turbine (T1) is mixed with the working fluid from the WFPUMP-1 in DCH and mixer. So, the discharge pressure of WFPUMP-1 is set to have the same value with T1 discharge pressure.

In addition, four binary variables are used to decide optimal process configuration. In the superstructure, the selections of alternatives are modeled as mixers, splitters and stream selectors. The vapor flash process configuration is available only when the WF-5 has a vapor fraction. The critical value of WFPUMP-1 discharge pressure

for this condition is 17.6 bar. In other words, the vapor flash process configuration is available only when the pressure of WF-5 is lower than 17.6 bar with MSCHE and 2-stage expansion configuration.

When the value of WFPUMP-1 discharge pressure is larger than 34.7 bar, liquid fraction starts to be generated in the low-pressure turbine (T2, T3) outlet streams. Thus, the value of WFPUMP-1 discharge pressure has an upper bound of 34.7 bar.

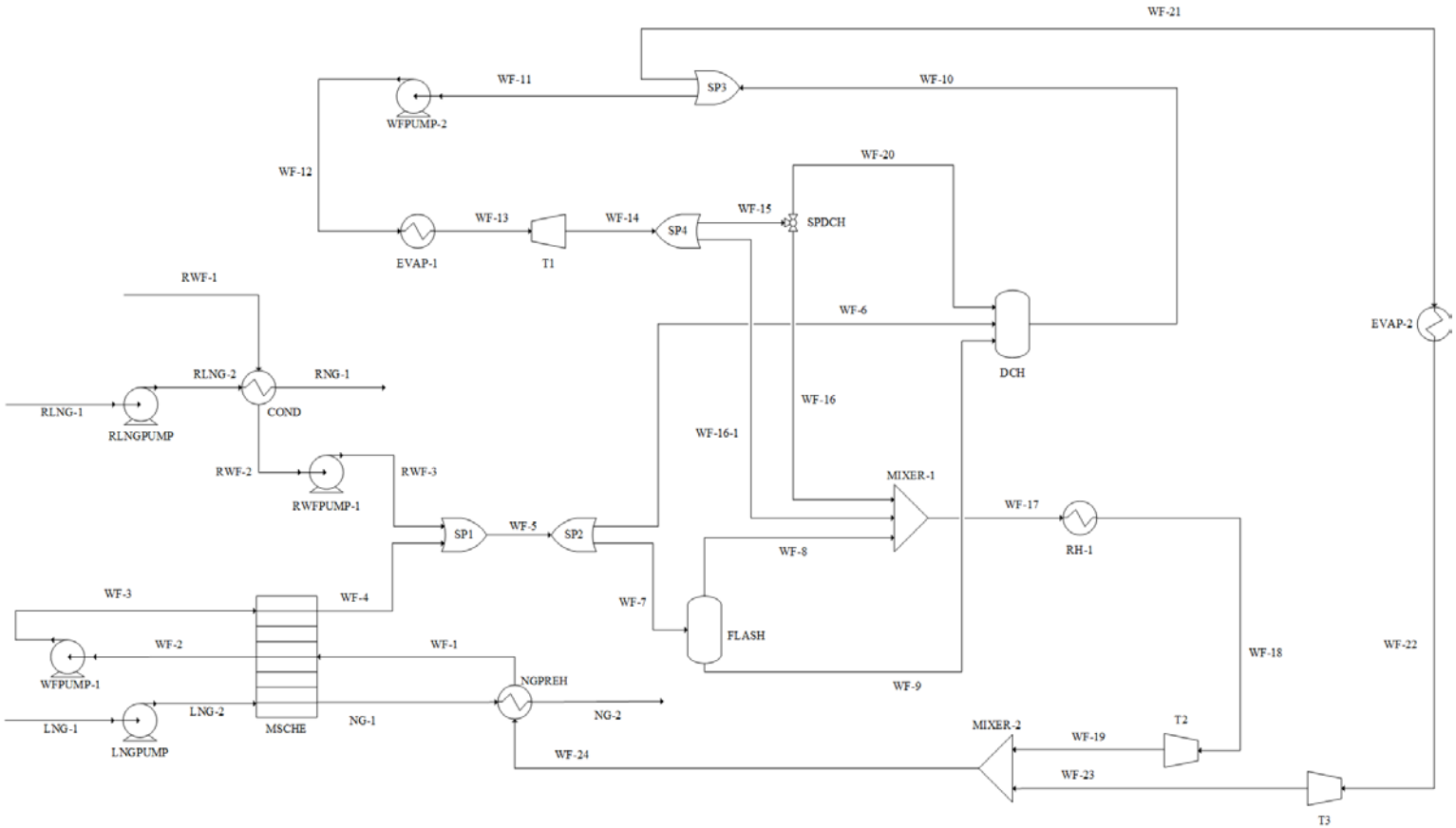

Figure 2-2. Superstructure of ORC process

Table 2-3. Input parameters and decision variables

Input Parameters	Value	Unit
Working fluid inlet pressure	1.6	bar
Minimum temperature approach of HXs	5	°C
Outlet temperature of the evaporators (EVAP-1, EVAP-2)	95	°C
Outlet temperature of the reheater (RH-1)	95	°C
Decision Variables	Lower bound	Upper bound
Continuous variables		
Discharge pressure of the first working fluid pump ($P_{WFPUMP-1}$)	5 bar	34.7 bar
Discharge pressure of the second working fluid pump ($P_{WFPUMP-2}$)	17.6 bar	90 bar
Binary variables		
SP1	0	1
SP2	0	1
SP3	0	1
SP4	0	1

CHAPTER 3 : Optimization Formulation

3.1. Formulation of optimization problem and constraints

The superstructure optimization of the ORC can be formulated as a MINLP problem.

$$\min f(x,y)$$
$$subject\ to \quad g_i(x,y) \le 0, \quad i = 1,2,3,\ldots..,p$$
$$h_j(x,y) = 0, \quad j = 1,2,3,\ldots..,q$$
$$x \in X \subset R^n, \quad y \in \{0,1\}^m \qquad \text{(P)}$$

where x and y are vectors consisting of n continuous and m integer variables. $f(x,y)$, $g(x,y)$, and $h(x,y)$ represent objective function, inequality, and equality constraints, respectively. Because the equality constraints are calculated in the process simulator or in objective function m-file, the original problem, P, can be expressed using penalty method.

$$\min F(x,y) = f(x,y) + \gamma c(x,y)$$
$$subject\ to \quad g_k(x,y) \le 0, \quad k = 1,2,3,\ldots,S, \qquad k \subset i$$
$$x \in X \subset R^n, \quad y \in \{0,1\}^m \qquad \text{(R)}$$

γ is a penalty parameter (1e9) and $c(x,y)$ represents convergence of the process simulator. When the process simulator fails to converge for an individual, $c(x,y)$ returns 1 to activate the penalty term. Then, a large penalty value is added to an objective function value, so that the optimizer can exclude infeasible region and proceed to the optimum solution effectively. Otherwise, it becomes zero. The

MINLP problem R does not include equality constraints as they are externally calculated in the process simulator, thus MATLAB built in stochastic solvers can be used without modification. The superstructure optimization is carried out by minimizing total annualized cost (TAC) of the ORC and it is explicitly calculated using an m-file. We assumed 25 years of plant life time and 0.154 [45] for capital recovery factor for annualizing total capital investment cost. Both annualized investment cost and averaged annualized operating cost are calculated according to in Lee *et al.* However, cost information or function is not readily available for a turbine. Herein, we assumed $212 of capital cost investment for turbine per kW electricity generation after consulting with a procurement company.

Four binary variables i.e., SP1, SP2, SP3, and SP4 decide the optimum configuration of the flowsheet. Each variable switches on or off for the MSCHE, vapor flash, 2nd stage expansion, and vapor recondensation process. Split fractions of splitters SP2, SP3, and SP4 can be calculated using equation 1.

$$X = 0.9998 \times \mathrm{SP} + 0.0001 \quad (1)$$

where X indicates the split fraction. The simulation of superstructure flowsheet may confront convergence problems when a steam has zero flow rate and it may exclude feasible solution while the optimization. Herein, a small split fraction is used to prevent zero flow in streams.

Two continuous variables decide outlet pressure of pumps. The lower and upper bounds for continuous variables are decided based on the sensitivity analysis. The outlet pressure of WFPUMP-1 is decided using the equation 2.

$$P_{\mathrm{WFPUMP-1}} = 17.6 \times SP2 + P_{\mathrm{PUMP-1}} \quad (2)$$

where $P_{\mathrm{WFPUMP-1}}$ is the pressure of pump outlet. Note that the value of $P_{\mathrm{WFPUMP-1}}$ controls outlet pressure of both WFPUMP-1 and RWFPUMP1 to reduce the number of variables. The vapor flash process can be only effective when phase separation occurs which often requires iterative calculation resulting expensive calculation. Through the sensitivity calculation we obtained the highest pressure generating two phase (17.6 bar), thus the outlet pressure of the pump can be decided using equation 2. The upper bound of $P_{\mathrm{PUMP-1}}$ is decided 17.1 bar and the optimization results show optimal solutions are resigned within the range.

Two linear inequality constraints are used to describe relation among variables. The vapor recondensation process is only possible when WF-4 is subcooled because the working fluid directed to the second pump should be resigned in the liquid phase.

$$SP2 - SP4 \geq 0 \tag{3}$$

Equation 3 describes relationship between the SP2 and SP4. SP4 can have value of 1 only if SP2 is 1. The outlet pressure of the second pump, WFPUMP-2, is always higher than that of the first pump as described in equation 4.

$$P_{WFPUMP-2} - 17.6 \times SP2 - P_{PUMP-1} \geq 0 \tag{4}$$

Several nonlinear equality constraints are also arose from the superstructure. MINLP problem with nonlinear equality constraints often fail to find a decent solution using stochastic solver and usually far more populations/generations are required for the solver as compared with the one without them. As aforementioned, nonlinear equality constraints are imbedded in the process simulator as design spec, thus the MINLP problem can be formulated without using equality constraints. Three design specs are implanted to find the working fluid flow rates and split

fraction for vapor recondensation process.

$$\min\left(\Delta T_d(\dot{m}_{WF-1})\right) = 5, \quad d = 1 \ldots 100 \tag{5}$$

$$VF_{RWF-2}(\dot{m}_{RWF-1}) = 0 \tag{6}$$

$$VF_{WF-10}(SP_{SPDCH}) = 0 \tag{7}$$

Equation 5 describe that the minimum approach temperature of MSCHE is 5°C. The input specifications of LNG stream are fixed, thus the minimum temperature can be manipulated by varying mass flow rate of working fluid inside. The mass flow rate of the working fluid can be calculated by using the fact that working fluid outlet (RWF-2) is completely liquefied when MSCHE is not selected. Similar to eqn. 5, LNG has fixed specification and completely evaporated in COND. The equation 7 decide working fluid flowrate circulating vapor recondensation process. The more working fluid in the loop generally produces the more power. The amount of recycled vapor can be increased only until the second pump inlet stream become saturate. The split fraction of SPDCH is manipulated to saturate the WF-10. Detailed information is also provided as ASPEN INPUT FILE which provided in supporting information.

3.2. Optimization Structure

The MINLP problem containing highly non-convex constraints such as non-ideal flash calculation often requires very expensive calculation, thus stochastic solution algorithms are used to solve the problem. Although stochastic algorithms do not guarantee the global optimum solution, it is an attractive option [46], because derivatives or mathematical information of the models is not necessary. Herein GA

is used for solving the MINLP problem. Maximum 50 generations with 60 individuals for a population is defined. The tournament selection method is used to choose parents for the next generation. Single point crossover with different crossover fractions, one elite population, and Gaussian mutation are also implemented in the GA solver. The maximum population size and five stall generations are used for termination criteria. The GA solved the optimization problem for four times in order to compare the quality of solutions with different crossover fraction. As aforementioned, it cannot be guaranteed that the solution obtained is global optimal.

The platform has interface between Aspen Plus and MATLAB allowing the GA to access Aspen. The GA generates random individuals and each individual is sent to Aspen Plus through an ActiveX server to verify that the given individual is resigned within the feasible region. If the individual it a feasible solution it returns $c(x, y) = 0$, and consequent objective function value (i.e., TAC) is calculated in objective function m-file. Otherwise, $c(x, y) = 1$ and a large penalty value (1e9) is assigned for the objective value. This method cannot completely identify the entire feasible region, but solver can successfully avoid infeasible region. The GA receives the objective function value from the m-file and checks the termination criteria. In case the criteria are fulfilled, it terminates. If not, the GA creates a new generation by its three characteristic steps: selection, mutation, and recombination. The optimization structure is summarized and presented in Figure 3-1.

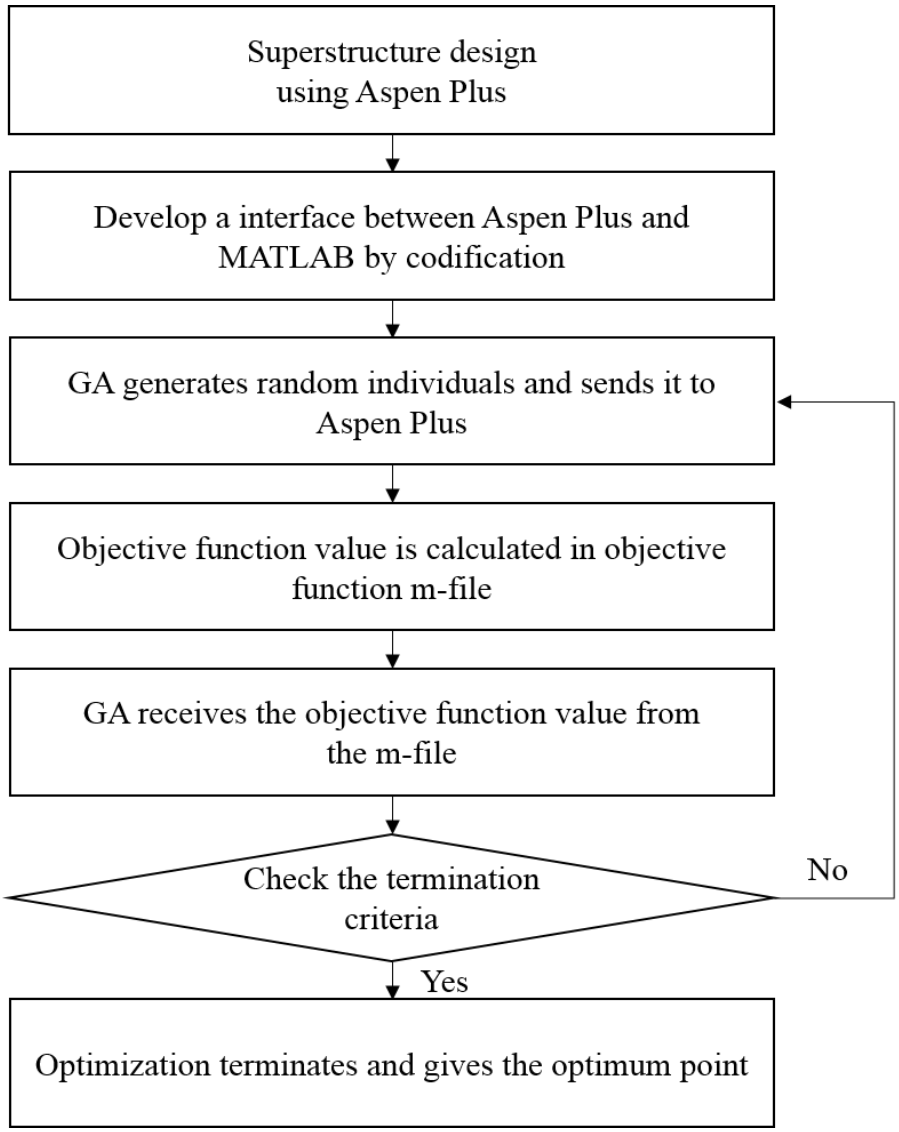

Figure 3-1. Flow chart of optimization

CHAPTER 4 : Results and Discussion

4.1. Results

Total four optimization execution results with different crossover fractions are summarized in Table 4-1. The results of GA evolution are showed in Figure 4-1 to 4-4. All four solutions show very similar net power generation and total annualized cost values. Among these, the first execution shows the best result. Figure 4-1 shows the result of GA execution with crossover fraction value of 0.4. GA is terminated at the 34th generation. The optimum ORC process configuration has MSCHE and 2-stage expansion, while vapor flash and VRP are not included. With this configuration, the optimal values of $P_{WFPUMP-1}$ and $P_{WFPUMP-2}$ are 18.5 bar and 79.8 bar respectively.

Through executions 1 to 4, the mean value of objective function is much larger than the best value. It is because of the penalty parameter which is set in the optimization problem formulation stage. When the process simulator fails to converge for an individual, a large penalty value is added to an objective function value. Thus, the optimizer can exclude infeasible region and proceed to the optimum solution effectively.

Table 4-1. Results of optimization of the ORC process

Execution	1	2	3	4
Gross power generation (GJ/h)	461.8	461.7	461.7	461.5
Pump work (GJ/h)	52.2	52.2	52.1	52.0
Net power generation (GJ/h)	409.6	409.6	409.6	409.5
Power generation per LNG (kJ/kg LNG)	252.8	252.8	252.8	252.8
Total annualized cost (M$/yr)	42.0	42.0	42.0	42.0
Continuous variables				
$P_{WFPUMP-1}$ (bar)	18.5	18.5	18.5	18.5
$P_{WFPUMP-2}$ (bar)	79.8	79.8	79.7	79.4
Binary variables				
MSCHE/COND (0 = MSCHE, 1 = COND)	0	0	0	0
Vapor flash (0 = yes, 1 = no)	1	1	1	1
2-Stage expansion (0 = no, 1 = yes)	1	1	1	1
VRP (0 = no, 1 = yes)	0	0	0	0
Crossover fraction	0.4	0.5	0.6	0.7
Number of generations	34	25	27	21
CPU time (s)	21012	15450	16686	12978

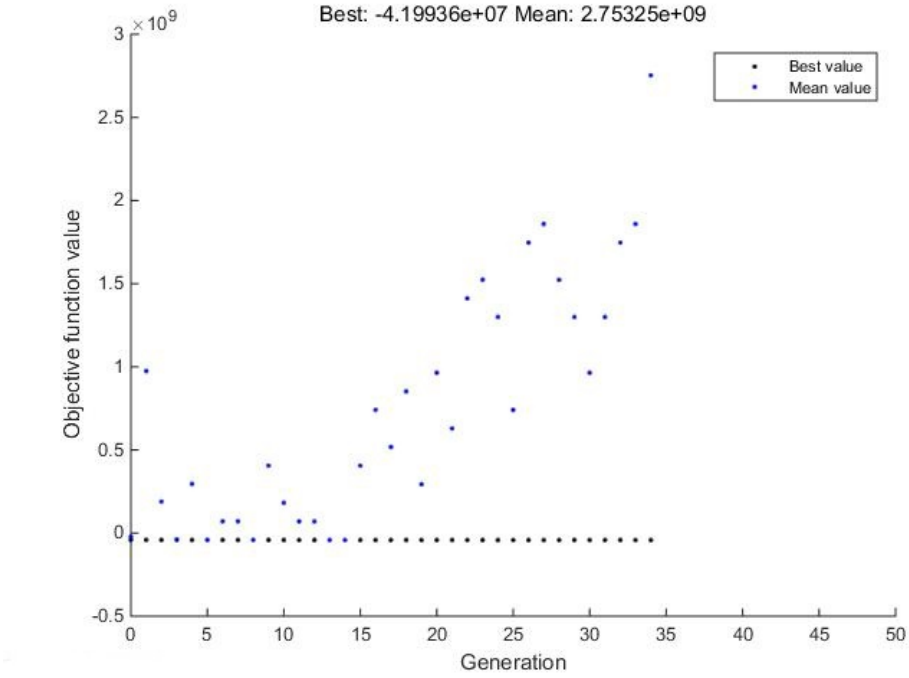

Figure 4-1. The result of GA evolution: execution 1

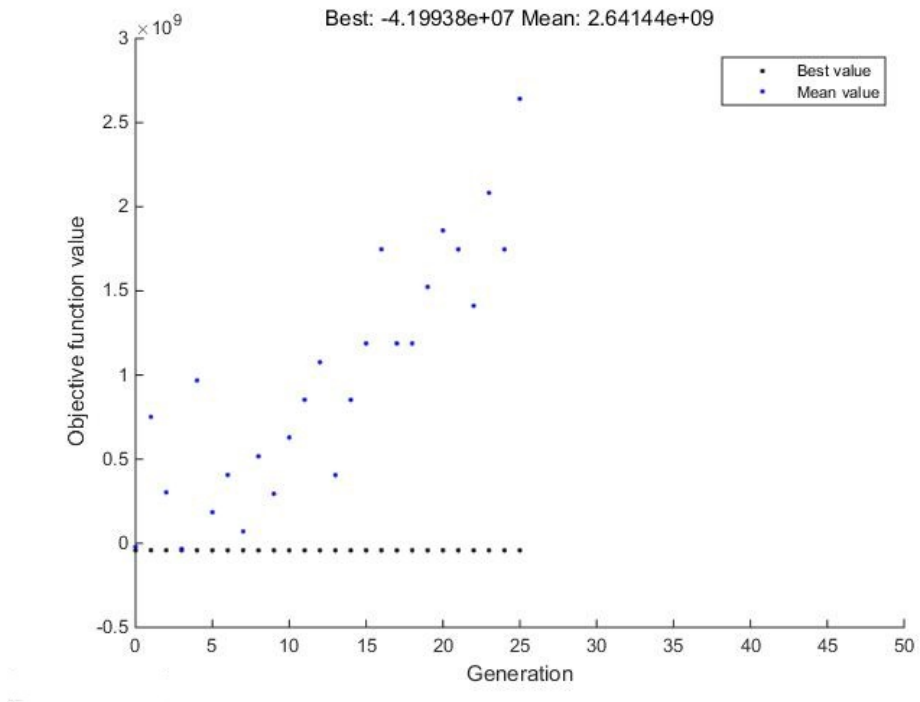

Figure 4-2. The result of GA evolution: execution 2

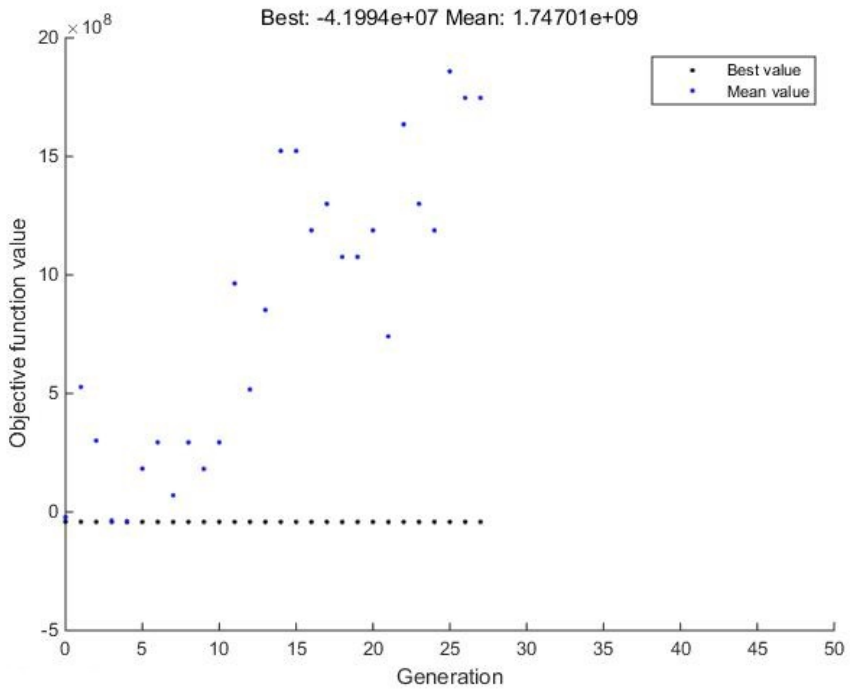

Figure 4-3. The result of GA evolution: execution 3

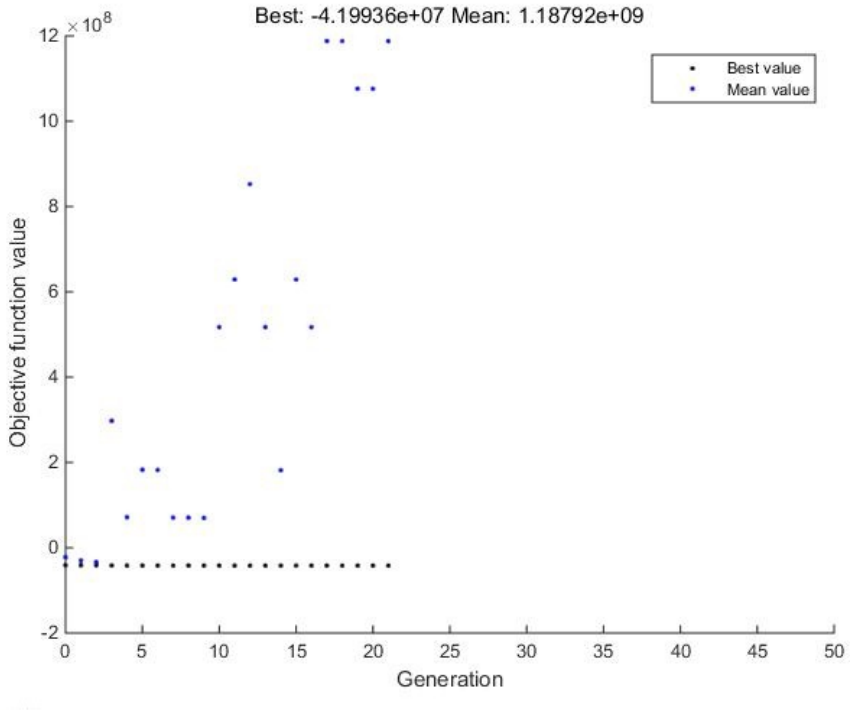

Figure 4-4. The result of GA evolution: execution 4

4.2. Discussion

The optimal configuration of ORC is compared with different configurations to verify whether the result is reliable or not. Figure 4-5 demonstrates the result of comparison. As shown in the figure, the net power generation and the power generation per kg of LNG are maximized with optimal configuration. When MSCHE is excluded from the optimal configuration, the amount of net power generation is decreased by 25.3 %. In the COND, only LNG is used as a heat sink for the condensation of the working fluid. On the other hand, the working fluid condensed in MSCHE can be used as a heat sink together with LNG. As a result, the amount of heat sink and the mass flow rate of the working fluid are increased with a fixed amount of LNG, and the amount of net power generation is increased also. The operating and capital cost of the process become more expensive by the adaptation of MSCHE. However, the profit of increased amount of net power generation compensates and surpasses the cost increment.

2-Stage expansion contributes on the amount of net power generation more than MSCHE. The amount of net power generation is decreased by 29.5 % when 1-stage expansion is adapted instead of 2-stage expansion. In the 1-stage expansion configuration, the exhausted stream from the turbine (T1) is sent back to the condensing procedure without reheating. This means that 1-stage expansion configuration cannot utilize the free heat source sufficiently. This eventually results in the decreased amount of net power generation. 1-stage expansion can reduce the operational and capital cost, but the power deration caused by 1-stage expansion has a more dominant effect on the cycle efficiency.

In the base case ORC process, 243.4 GJ/h of net power is generated, and it is

equivalent to 150.3 kJ/kg LNG. The optimum configuration of ORC generates 68.2 % more power per kg of LNG than the base case.

Sensitivity analysis was also carried out to verify reliability of optimization result. Continuous variables, $P_{WFPUMP-1}$ and $P_{WFPUMP-2}$, are used for sensitivity analysis. The results of sensitivity analysis are shown in Figure 4-6 and 4-7. Figure 4-6 shows a sensitivity analysis of the $P_{WFPUMP-1}$ on the net power generation and the profit. As shown in the figure, the net power generation and the profit is maximized with the optimal value of $P_{WFPUMP-1}$ (18.5 bar). When the pressure is less than optimal value, vapor fraction is generated in the stream WF-5, thus the optimum process configuration cannot be adapted. Figure 4-7 shows a sensitivity analysis of the $P_{WFPUMP-2}$ on the net power generation and the profit. Although the net power generation increases as the PWFPUMP-2 gets high, the profit decreases when the $P_{WFPUMP-2}$ exceeds optimal value (79.8 bar). This is because the operating and capital cost of the process is increased. When the value of $P_{WFPUMP-2}$ exceeds optimal value, the increment of profit caused by increased power generation cannot overcome the increment of operating and capital cost of the process.

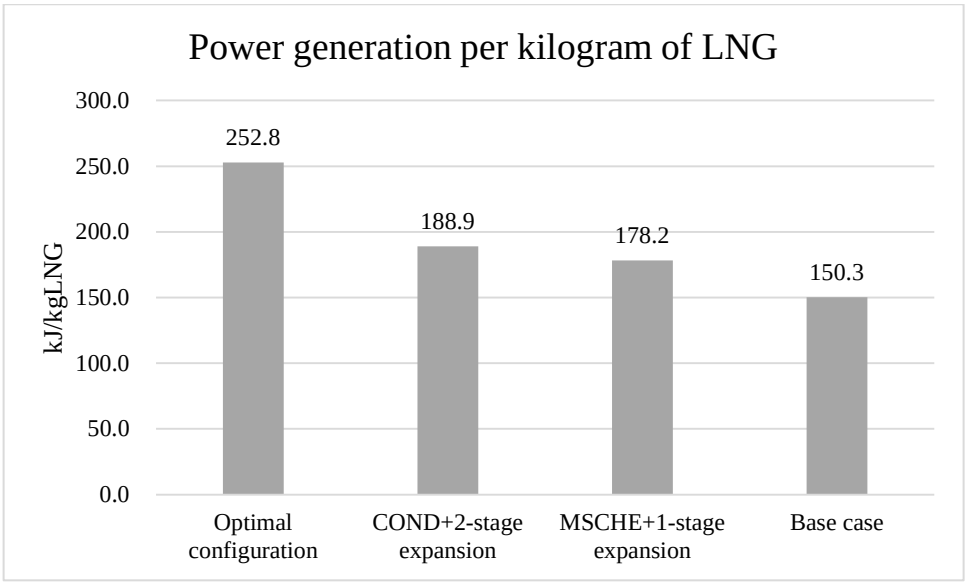

Figure 4-5. Power generation of representative process configurations in superstructure

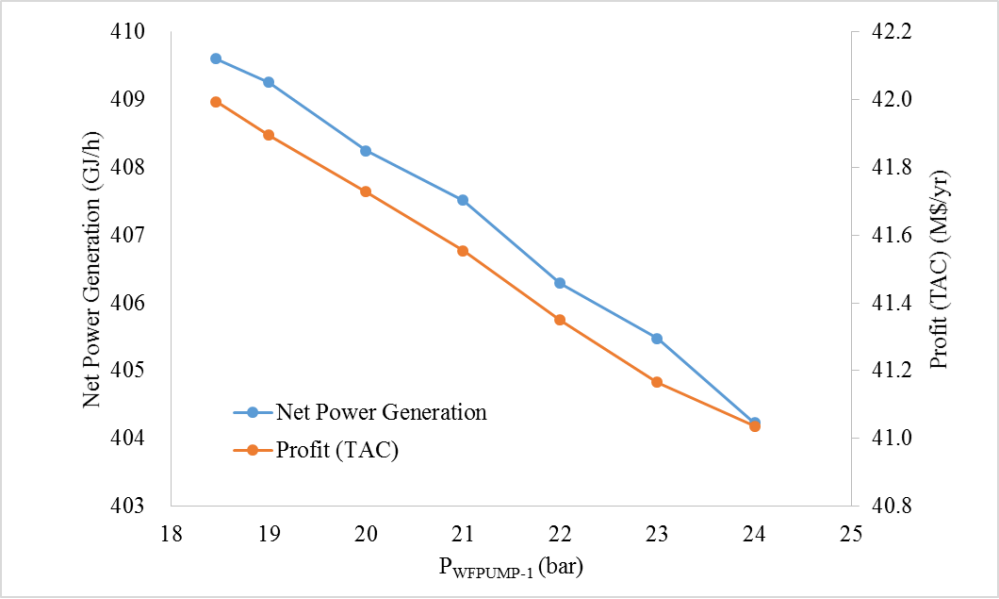

Figure 4-6. Result of sensitivity analysis for $P_{WFPUMP-1}$

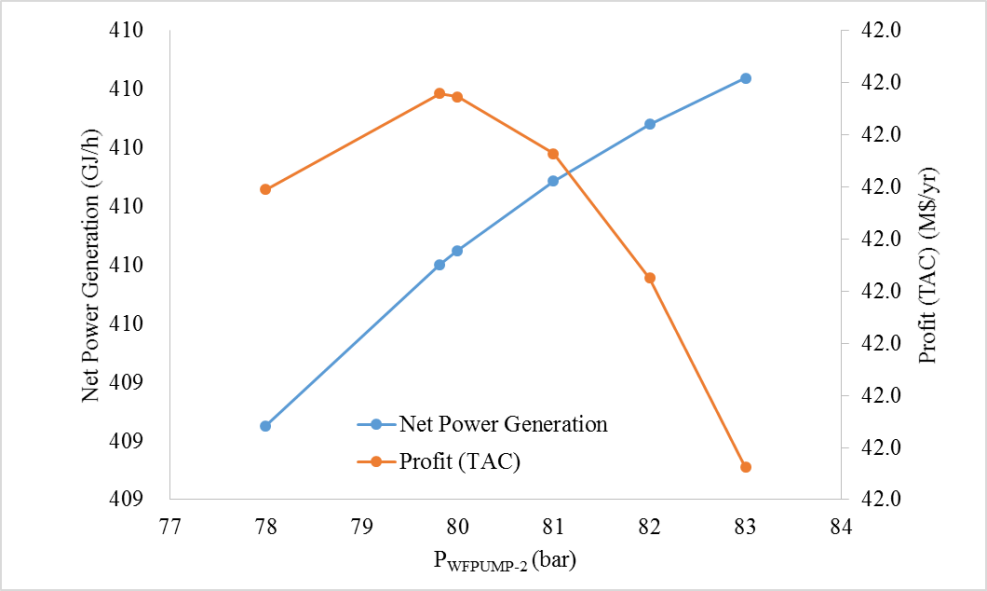

Figure 4-7. Result of sensitivity analysis for $P_{WFPUMP-2}$

CHAPTER 5 : Modeling and Design of Vapor Recovery Unit (VRU) Processes on Carrier Ship

5.1. Introduction

In the previous chapters, an optimal ORC process utilizing LNG cold energy is proposed by superstructure optimization. LNG is used as a heat sink in the proposed ORC process. LNG is mainly transported from production site to terminal by carrier ship.

As International Maritime Organization (IMO) obliged the reduction of the quantity of emission of VOCs (Volatile Organic Compounds) from the ship, the necessity of installing SVRU (Ship Vapor Recovery Unit) has been increased.

For this reason, lots of researches for effective recovery of VOCs on tanker ship that carries petroleums product are ongoing. In the SVRU process, recovered VOCs are reused as a fuel, so it is beneficial both in environmental and economic aspects. Recently, main commercial SVRU processes utilize the method of absorption, adsorption, membrane separation, and cryogenic condensation.

In this chapter, a model of SVRU process that utilize absorption and membrane separation was developed using Aspen Plus. This process recovers VOCs using absorption with heptane (C7) absorbent, seawater heat exchange, and membrane separation. Based on the developed model, modified conceptual design of SVRU was proposed to improve VOC recovery efficiency and energy consumption of the process.

5.2. Process description

Vapor recovery unit (VRU) process consists of scrubber, compressor, heat exchanger, flash drum, and membrane separator. Among components of VOCs, heavy components like pentane (C5), hexane (C6), and heptane (C7) are recovered by the scrubber. And then, propane (C3) and butane (C4) are recovered by the compressor and heat exchanger. Finally, the light components, methane (C1) and ethane (C2), are recovered by the membrane separator. Recovered VOCs are sent to the storage tank and used as a fuel.

Process modeling is performed using Aspen Plus. PSRK (Predictive Soave-Redlich-Kwong) is selected as a physical property method. Because it is known proper to the light hydrocarbon system.

The feed stream of this process is VOCs from the ship. The composition of VOCs can be changed by types of oil or gas, and environmental factors. In this chapter, the fixed composition of VOCs are used. This composition of VOCs are provided from a procurement company. The condition and composition of the VOCs are presented in Table 5.1 and 5.2.

Table 5-1. Condition of the feed stream

Volatile Organic Gas Feed	Vapor Fraction	1.00
	Temperature (°C)	45.0
	Pressure (barg)	0.15
	Volumetric Flow (cum/hr)	2000

Table 5-2. Composition of the feed stream

Component	Composition (mol%)	Total composition (mol%)
Methane	0.20	Hydrocarbon 30
Ethane	1.55	
Propane	7.06	
i-Butane	6.98	
n-Butane	4.92	
i-Pentane	1.84	
n-Pentane	1.88	
2-methyl Pentane	0.64	
3-methyl Pentane	0.25	
Hexane	0.64	
other HC(Heptane)	4.04	
CO_2	12.00	Inert Gas 70
N_2	58.00	
Total	100	100

5.3. Process modeling

The developed model of SVRU process is depicted in Figure 5-1. At the first stage, the VOCs feed stream is flowed in the scrubber. Heavy hydrocarbons (> C5) are absorbed by C7 absorbent in the scrubber, and recovered from the bottom of the scrubber. Remaining hydrocarbons in the top stream of the scrubber are sent to the compressor. At the compressor, VOCs are pressurized to 9.7 bar and sent to the heat exchanger. Pressurized VOCs are refrigerated to 15.4 °C by sea water (5 °C) in the heat exchanger. After pressurization and refrigeration, VOCs are flashed in the flash drum. Hydrocarbons over C3 are recovered from the bottom of the flash drum. Finally, remaining light hydrocarbons (C1 and C2) are recovered at the membrane separator.

In the compressor, discharge pressure cannot exceed 10 bar because of the process characteristic. SVRU process is located on the ship, so that the operation in very high-pressure region is not available. In addition, the recovery ratio of membrane separator is assumed to 50 %, because of lack of detail data.

The results of modeling and simulation is presented in Table 5-3 to 5-6. The result showed that recovery ratio of hydrocarbons is 90.47 %.

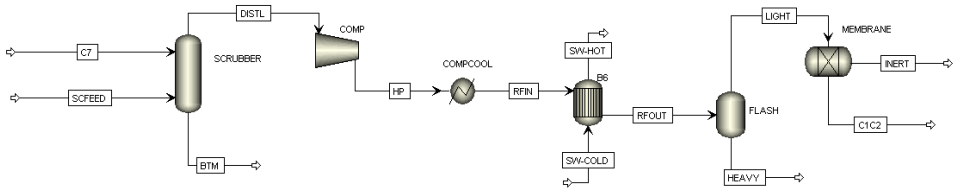

Figure 5-1. Process flow diagram of SVRU process

Table 5-3. Stream table of the SVRU process

	Feed Stream	C7 Absorbent	Scrubber outlet - liquid	Flash outlet - liquid	Membrane outlet - HC	Membrane outlet - Inert
Temperature [℃]	45	25	30.1	15	15	15
Pressure [bar]	1.163	1.013	1.013	9.7	9.7	9.7
Vapor Frac	1	0	0	0	0	1
Mole Flow [kmol/hr]	88.331	37.523	38.415	13.89	6.101	67.449
Mass Flow [kg/hr]	3542.781	3759.945	3713.488	1091.822	307.234	2190.182
Volume Flow [cum/hr]	2000	6.300	6.289	1.876	0.614	164.415
Enthalpy [Gcal/hr]	-1.824	-2.011	-1.995	-0.639	-0.199	-1.144
Mole Flow [kmol/hr]						
Methane	0.177	0	0	0.002	0.087	0.087
Ethane	1.369	0	0.017	0.081	0.636	0.636
Propane	6.236	0	0.279	1.179	2.389	2.389
i-Butane	6.166	0	0.677	2.118	1.685	1.685
n-Butane	4.346	0	0.687	1.753	0.953	0.953
i-Pentane	1.625	0	0.618	0.71	0.148	0.148
n-Pentane	1.661	0	0.81	0.649	0.1	0.1
2-Methyl pentane	0.565	0	0.464	0.09	0.006	0.006
3-Methyl pentane	0.221	0	0.187	0.03	0.002	0.002
n-Hexane	0.565	0	0.511	0.05	0.002	0.002
n-Heptane	3.569	37.523	34.079	6.828	0.092	0.092
CO2	10.6	0	0.056	0.268	0	10.276
N2	51.232	0	0.029	0.132	0	51.072

Table 5-4. Recovery ratio of hydrocarbons (exclude C7)

Recovered hydrocarbon	Scrubber bottom	18.53%
	Flash drum bottom	29.05%
	Membrane outlet	26.20%
	Total	73.79%
Non recovered hydrocarbon	Total	26.20%

Table 5-5. Recovery ratio of hydrocarbons (include C7)

Recovered hydrocarbon	Scrubber bottom	59.87%
	Flash drum bottom	21.07%
	Membrane outlet	9.53%
	Total	90.47%
Non recovered hydrocarbon	Total	9.53%

Table 5-6. Recovery ratio of each component of hydrocarbons

Component	Inlet [kmol/hr]	Outlet [kmol/hr]		Recovery ratio [%]
		Non recovered	Recovered	
Methane (C1)	0.1767	0.0874	0.0893	50.54%
Ethane (C2)	1.3691	0.6356	0.7335	53.58%
Propane (C3)	6.2362	2.3891	3.8471	61.69%
i-Butane (iC4)	6.1655	1.6853	4.4803	72.67%
n-Butane (nC4)	4.3459	0.9526	3.3933	78.08%
i-Pentane (iC5)	1.6253	0.1485	1.4768	90.86%
n-Pentane (nC5)	1.6606	0.1005	1.5602	93.95%
2-Methyl pentane (C6)	0.5653	0.0058	0.5596	98.99%
3-Methyl pentane (C6)	0.2208	0.0017	0.2191	99.23%
n-Hexane (C6)	0.5653	0.0023	0.5631	99.60%
n-Heptane (C7)	41.0915	0.0922	40.9993	99.78%

The recovery ratios of heavy hydrocarbons (C5 to C7) are achieved over 90 %. However, mole fraction of heavy hydrocarbon to entire hydrocarbon is only 31 %. The recovery ratios of C1 and C2 have the value of near 50 %. It is very low level of recovery performance, but has not significant effect on entire system performance. Because mole fraction of C1 and C2 is only 3 %.

C3 and C4 comprise 63 % of mole fraction, and its recovery ratio is 60 – 78 %. The recovery ratios of C3 and C4 are the most important factor for the entire process efficiency. C3 and C4 are mainly recovered in compression/refrigeration system.

5.4. Process alternative for improving efficiency

Process alternative is proposed in this section to improve recovery ratio and energy consumption of the process. In the original process configuration, there is one membrane separator at the latter part of the process. The proposed process configuration has one more membrane separator between scrubber and compressor. Remaining hydrocarbons in the top stream of the scrubber are sent to the membrane separator instead of compressor. The proposed process is depicted in Figure 5-2, and the results are presented in Table 5-7 and 5-8.

As shown in Table 5-7, overall recovery ratio of each component is improved by adding an additional membrane separator. Entire recovery ratio of the process is increase from 90.5 % to 94.1 %. Moreover, energy consumption of compressor is reduced in the proposed process configuration, because the flow rate of VOCs is decreased by adding an additional membrane separator before the compressor. The amount of decreased energy consumption 10.93 %, and the result is showed in Table 5-9.

Consequently, proposed process alternative shows improved recovery ratio of VOCs and energy consumption of compressor compared to the base case.

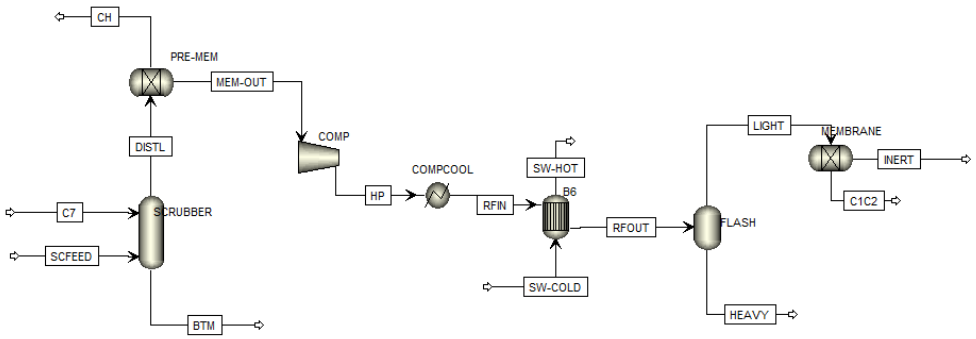

Figure 5-2. Process flow diagram of modified SVRU process

Table 5-7. The result of modified process

Component	Feed Stream	Scrubber Outlet-liquid	Mem -Outlet (1)	Flash Outlet-liquid	Mem -Outlet (2)	Recovery ratio [%]
Methane [kmol/hr]	0.176	3.37E-04	0.088	0	0.087	74.58
Ethane [kmol/hr]	1.369	0.016	0.676	0.081	0.635	75.89
Propane [kmol/hr]	6.236	0.279	2.979	1.178	2.389	78.34
i-Butane [kmol/hr]	6.165	0.676	2.744	2.118	1.685	82.34
n-Butane [kmol/hr]	4.345	0.687	1.829	1.754	0.952	84.79
i-Pentane [kmol/hr]	1.625	0.618	0.503	0.709	0.148	92.25
n-Pentane [kmol/hr]	1.660	0.811	0.425	0.649	0.100	94.52
2-Methyl pentane [kmol/hr]	0.565	0.463	0.051	0.090	0.006	99.12
3-Methyl pentane [kmol/hr]	0.220	0.187	0.017	0.029	0.002	99.10
n-Hexane [kmol/hr]	0.565	0.510	0.027	0.049	0.002	99.47
n-Heptane [kmol/hr]	3.568	34.076	3.506	6.827	0.092	99.74

Table 5-8. Comparison of recovery ratio between base case and proposed process alternative

Process	Recovery ratio [%] (exclude C7)	Recovery ratio [%] (include C7)
Base case	73.8	90.5
Proposed process	83.9	94.1

Table 5-9. Comparison of energy consumption between base case and proposed process alternative

Process	Compressor power [kW]
Base case	226.907
Proposed process	202.117

CHAPTER 6 : Conclusion and Future Works

6.1. Conclusion

In this thesis, an optimal ORC process utilizing LNG cold energy is proposed. The ORC process is modeled using Aspen Plus™ v7.3. The Peng-Robinson equation of state is used to calculate the thermodynamic properties and phase behavior of the ORCs. The working fluid of the ORC is composed of normal pentane, trifluoromethane, and tetrafluoromethane. The optimization of the process to minimize total annualized cost (TAC) is performed using superstructure based approach. The developed superstructure includes four process alternatives, which are MSCHE, vapor flash process, 2-stage expansion, and VRP. The optimum solution is attained using the Aspen Plus-interface-MATLAB GA optimizer structure. The optimum ORC process configuration has MSCHE and 2-stage expansion. With this configuration, the optimal values of $P_{WFPUMP-1}$ and $P_{WFPUMP-2}$ are 18.5 and 79.8 respectively. The optimal process shows the net power generation of 409.6 GJ/h, and the power generation per unit kilogram of LNG is increased by 68.2 %.

Additionally, modeling of ship vapor recovery unit, which can be adapted to LNG or crude oil carrier ship, is performed. Overall process efficiency including VOCs recovery ratio and energy consumption is increased by the proposed process alternative.

6.2. Future works

The proposed ORC process shows good performance, but still several topics can be suggested for future works. In this thesis, the waste heat of 100 °C is used as a heat source. The developed superstructure and optimization problem can be applied to other heat sources, which have lower or higher temperatures. As a quality of a heat source, different result of optimization can be deduced.

The fixed working fluid composition is used in this study. However, simultaneous optimization of working fluid and process configuration can be adopted. Through simultaneous optimization, the composition or the type of substances of working fluid can be changed. Although it often requires enormous calculation time and fails to global optimum solution, it may deduce improved result. To find the global optimum ORC process configuration, deterministic global optimization can be performed also. Finally, process safety issues, which have been receiving attention nowadays, can be considered to obtain a safer process design.

References

[1] Jing L, Zhihong L, Ben H. Current Status and Developing Prospect of LNG Cryogenic Energy Utilization. Natural Gas Industry. 2005;25:103.

[2] Tchanche BF, Lambrinos G, Frangoudakis A, Papadakis G. Low-grade heat conversion into power using organic Rankine cycles – A review of various applications. Renewable and Sustainable Energy Reviews. 2011;15:3963-79.

[3] He S, Chang H, Zhang X, Shu S, Duan C. Working fluid selection for an Organic Rankine Cycle utilizing high and low temperature energy of an LNG engine. Applied Thermal Engineering. 2015;90:579-89.

[4] Saleh B, Koglbauer G, Wendland M, Fischer J. Working fluids for low-temperature organic Rankine cycles. Energy. 2007;32:1210-21.

[5] Bao J, Zhao L. A review of working fluid and expander selections for organic Rankine cycle. Renewable and Sustainable Energy Reviews. 2013;24:325-42.

[6] Wang EH, Zhang HG, Fan BY, Ouyang MG, Zhao Y, Mu QH. Study of working fluid selection of organic Rankine cycle (ORC) for engine waste heat recovery. Energy. 2011;36:3406-18.

[7] Liu B-T, Chien K-H, Wang C-C. Effect of working fluids on organic Rankine cycle for waste heat recovery. Energy. 2004;29:1207-17.

[8] Hung TC, Wang SK, Kuo CH, Pei BS, Tsai KF. A study of organic working fluids on system efficiency of an ORC using low-grade energy sources. Energy. 2010;35:1403-11.

[9] Cataldo F, Mastrullo R, Mauro AW, Vanoli GP. Fluid selection of Organic Rankine Cycle for low-temperature waste heat recovery based on thermal optimization. Energy. 2014;72:159-67.

[10] Rayegan R, Tao YX. A procedure to select working fluids for Solar Organic Rankine Cycles (ORCs). Renewable Energy. 2011;36:659-70.

[11] Meinel D, Wieland C, Spliethoff H. Effect and comparison of different working fluids on a two-stage organic rankine cycle (ORC) concept. Applied Thermal Engineering. 2014;63:246-53.

[12] Maizza V, Maizza A. Unconventional working fluids in organic Rankine-cycles for waste energy recovery systems. Applied thermal engineering. 2001;21:381-90.

[13] Liu Y, Guo K. A novel cryogenic power cycle for LNG cold energy recovery. Energy. 2011;36:2828-33.

[14] Kim K, Lee U, Kim C, Han C. Design and optimization of cascade organic Rankine cycle for recovering cryogenic energy from liquefied natural gas using binary working fluid. Energy. 2015;88:304-13.

[15] Sun H, Zhu H, Liu F, Ding H. Simulation and optimization of a novel Rankine power cycle for recovering cold energy from liquefied natural gas using a mixed working fluid. Energy. 2014;70:317-24.

[16] Shi X, Che D. A combined power cycle utilizing low-temperature waste heat and LNG cold energy. Energy Conversion and Management. 2009;50:567-75.

[17] Wang J, Yan Z, Wang M, Dai Y. Thermodynamic analysis and optimization of an ammonia-water power system with LNG (liquefied natural gas) as its heat sink. Energy. 2013;50:513-22.

[18] Lee U, Kim K, Han C. Design and optimization of multi-component organic rankine cycle using liquefied natural gas cryogenic exergy. Energy. 2014;77:520-32.

[19] Heberle F, Preißinger M, Brüggemann D. Zeotropic mixtures as working fluids in Organic Rankine Cycles for low-enthalpy geothermal resources. Renewable Energy. 2012;37:364-70.

[20] Mavrou P, Papadopoulos AI, Stijepovic MZ, Seferlis P, Linke P, Voutetakis S.

Novel and conventional working fluid mixtures for solar Rankine cycles: Performance assessment and multi-criteria selection. Applied Thermal Engineering. 2015;75:384-96.

[21] Papadopoulos AI, Stijepovic M, Linke P. On the systematic design and selection of optimal working fluids for Organic Rankine Cycles. Applied Thermal Engineering. 2010;30:760-9.

[22] Lecompte S, Huisseune H, van den Broek M, Vanslambrouck B, De Paepe M. Review of organic Rankine cycle (ORC) architectures for waste heat recovery. Renewable and Sustainable Energy Reviews. 2015;47:448-61.

[23] Roy JP, Mishra MK, Misra A. Parametric optimization and performance analysis of a waste heat recovery system using Organic Rankine Cycle. Energy. 2010;35:5049-62.

[24] Lee U, Park K, Jeong YS, Lee S, Han C. Design and Analysis of a Combined Rankine Cycle for Waste Heat Recovery of a Coal Power Plant Using LNG Cryogenic Exergy. Industrial & Engineering Chemistry Research. 2014;53:9812-24.

[25] Zhao L, Dong H, Tang J, Cai J. Cold energy utilization of liquefied natural gas for capturing carbon dioxide in the flue gas from the magnesite processing industry. Energy. 2015.

[26] Madhawa Hettiarachchi HD, Golubovic M, Worek WM, Ikegami Y. Optimum design criteria for an Organic Rankine cycle using low-temperature geothermal heat sources. Energy. 2007;32:1698-706.

[27] Li P, Li J, Pei G, Munir A, Ji J. A cascade organic Rankine cycle power generation system using hybrid solar energy and liquefied natural gas. Solar Energy. 2016;127:136-46.

[28] Chen H, Goswami DY, Stefanakos EK. A review of thermodynamic cycles and working fluids for the conversion of low-grade heat. Renewable and Sustainable

Energy Reviews. 2010;14:3059-67.

[29] Lee U, Han C. Simulation and optimization of multi-component organic Rankine cycle integrated with post-combustion capture process. Computers & Chemical Engineering. 2015;83:21-34.

[30] Desai NB, Bandyopadhyay S. Process integration of organic Rankine cycle. Energy. 2009;34:1674-86.

[31] Mago PJ, Chamra LM, Srinivasan K, Somayaji C. An examination of regenerative organic Rankine cycles using dry fluids. Applied Thermal Engineering. 2008;28:998-1007.

[32] Pei G, Li J, Ji J. Analysis of low temperature solar thermal electric generation using regenerative Organic Rankine Cycle. Applied Thermal Engineering. 2010;30:998-1004.

[33] Xu R-J, He Y-L. A vapor injector-based novel regenerative organic Rankine cycle. Applied Thermal Engineering. 2011;31:1238-43.

[34] Edrisi BH, Michaelides EE. Effect of the working fluid on the optimum work of binary-flashing geothermal power plants. Energy. 2013;50:389-94.

[35] Ho T, Mao SS, Greif R. Comparison of the Organic Flash Cycle (OFC) to other advanced vapor cycles for intermediate and high temperature waste heat reclamation and solar thermal energy. Energy. 2012;42:213-23.

[36] Ho T, Mao SS, Greif R. Increased power production through enhancements to the Organic Flash Cycle (OFC). Energy. 2012;45:686-95.

[37] Tomków Ł, Cholewiński M. Improvement of the LNG (liquid natural gas) regasification efficiency by utilizing the cold exergy with a coupled absorption – ORC (organic Rankine cycle). Energy. 2015;87:645-53.

[38] Lampe M, Stavrou M, Bücker HM, Gross J, Bardow A. Simultaneous Optimization of Working Fluid and Process for Organic Rankine Cycles Using PC-

SAFT. Industrial & Engineering Chemistry Research. 2014;53:8821-30.

[39] Grossmann IE. Mixed-integer programming approach for the synthesis of integrated process flowsheets. Computers & chemical engineering. 1985;9:463-82.

[40] Grossmann IE. MINLP optimization strategies and algorithms for process synthesis. 1989.

[41] Grossmann IE. Mixed-integer nonlinear programming techniques for the synthesis of engineering systems. Research in Engineering Design. 1990;1:205-28.

[42] Peng D-Y, Robinson DB. A new two-constant equation of state. Industrial & Engineering Chemistry Fundamentals. 1976;15:59-64.

[43] Bowen RR, Cole ET, Kimble EL, Thomas ER, Kelley LR. Multi-component refrigeration process for liquefaction of natural gas. Google Patents; 1999.

[44] Park C, Song K, Lee S, Lim Y, Han C. Retrofit design of a boil-off gas handling process in liquefied natural gas receiving terminals. Energy. 2012;44:69-78.

[45] Hasan MF, Baliban RC, Elia JA, Floudas CA. Modeling, simulation, and optimization of postcombustion CO2 capture for variable feed concentration and flow rate. 1. Chemical absorption and membrane processes. Industrial & Engineering Chemistry Research. 2012;51:15642-64.

[46] Leboreiro J, Acevedo J. Processes synthesis and design of distillation sequences using modular simulators: a genetic algorithm framework. Computers & Chemical Engineering. 2004;28:1223-36.

Abstract in Korean (국문요약)

액화천연가스(LNG)는 높은 에너지 밀도와 적은 양의 온실가스 배출량 등의 장점으로 인해 에너지원으로 주목 받고 있다. 산지에서 수입된 LNG 는 터미널에서 기화 과정을 거쳐 최종 소비자에게 공급된다. 일반적으로 LNG 는 터미널에서 해수를 이용해 기화되는데, 이 때 LNG 가 가지고 있는 냉열은 활용되지 못하고 대부분 버려지고 있는 실정이다. LNG 가 가지고 있는 냉열을 버리는 대신, 유기 랭킨 사이클(organic Rankine cycle, ORC)의 히트 싱크로 활용하면 전력 생산이 가능해져 이윤을 창출할 수 있다. 이러한 ORC 의 공정 설계와 최적화에 대한 연구가 공정의 효율 및 경제성을 향상시키기 위해 최근 활발히 진행되고 있다. 본 논문에서는 LNG 의 냉열을 활용하는 다 성분 작동 유체 ORC 의 최적 설계를 제시한다. ORC 의 전력 생산량을 증대시키고, 공정의 건설 비용 및 운전 비용을 절감할 수 있는 공정 개선안들을 제안 및 적용하여 ORC 의 초구조체 (superstructure)를 개발하였다. 적용된 공정 개선안들은 다중 흐름 초저온 열 교환기 (Multi-stream cryogenic heat exchanger), 증기 플래시 공정, 2 단 팽창 공정, 증기 재응축 공정이다. 상용 공정 모사기를 이용하여 ORC 초구조체를 모델링 하였으며, 개발된 초구조체의 최적화는 혼합 정수 계획법 중의 하나인 유전 알고리즘을 이용하여 공정의 총 연간비용을 최소화 하는 방향으로 수행되었다. 공정 개선안들의 선택여부를 결정하는 4 개의 2 진 변수와, 공정의 운전 조건인 작동 유체 펌프의 압축 압력을 나타내는 2 개의 연속 변수를 이용해 최적화를 수행한 결과, 다중 흐름

초저온 열 교환기와 2 단 팽창 공정이 적용되었을 때가 최적 공정 구성인 것으로 나타났다. 도출된 최적 공정 구성과 최적 운전 조건에서 LNG 의 단위 kg 당 ORC 의 전력 생산량은 약 68.2% 향상된 결과를 보였다. 본 연구의 결과를 통해, 현재 활용되지 못하고 있는 액화천연가스의 냉열을 전력 생산에 활용함으로써 에너지 절감 및 경제적 이익 창출에 기여할 수 있을 것으로 기대된다.

주요어: 액화천연가스, 다성분 작동유체, 유기 랭킨 사이클, 초구조체, 유전 알고리즘

학번: 2009-21023
성명: 전 정 우